



Assessment of coupled CRCM5–FLake on the reproduction of wintertime lake-induced precipitation in the Great Lakes Basin

Janine A. Bajinath-Rodino¹ · Claude R. Duguay¹

Received: 18 May 2018 / Accepted: 27 January 2019 / Published online: 22 February 2019
© Springer-Verlag GmbH Austria, part of Springer Nature 2019

Abstract

This study assesses the high-resolution, 0.11° (12 km), Canadian Regional Climate Model Version 5 (CRCM5), interactively coupled to the one-dimensional Freshwater Lake model (FLake), to predict wintertime precipitation along the Canadian snowbelts of Lake Superior and Lake Huron. CRCM5–FLake was compared against various datasets to evaluate the 20-year (1995–2014) SWE and wintertime precipitation, seven lake-induced precipitation events and lake effect snowfall (LES) predictor variables during the months of December and January. The findings of SWE along both snowbelts in December and January show MBD ≤ -10 mm and ≤ -30 mm, respectively. Similarly, precipitation results along both snowbelts in December and January show MBD ≤ -5 mm and ≤ -10 mm, respectively. The negative biases in simulated SWE and precipitation, predominantly along the snowbelts, suggest that the model may un-realistically represent lake effect processes. Comparison of lake-induced precipitation events also indicates that the model mostly under-predicts the daily accumulated precipitation associated with each event but tends to accurately capture the timing and the general location of the squalls along the snowbelts, though not for highly localised snow bands. Furthermore, lake-wide results of LES predictor variables indicate that the model over-estimates lake surface temperature (LST) for both lakes during December and January and under-estimates ice cover concentrations for both lakes in December. The resultant biases could be attributed to limitations within the coupled RCM because the quality of reproducing lake-induced precipitation in this region is highly dependent on the performance of FLake.

1 Introduction

Lakes have profound effects on the regional climate and weather (Anyah and Semazzi 2004; Obolkinm and Potemkin 2006; Dupont et al. 2012; Martynov et al. 2012). Canada is the country with the most number of lakes (ECCC 2017). Over 500 of these lakes are larger than 100 km², with some of these lakes ranked among the largest, by area, worldwide (ECCC 2017). Their large spatial extent and geographic location make some of these lakes susceptible to lake effect snowfall (LES) during the cold season, such as the Laurentian Great Lakes (Notaro et al. 2013a, b), Lake Athabasca, Lake Winnipeg, Lake Winnipegosis (Carpenter 1993; Cairns et al. 2001; Payer et al. 2007; Laird et al. 2009, 2010; Hartmann et al. 2013), and the Great Bear and Great Slave Lake. With

cold and dry Arctic air advecting southward, the lake-rich country of Canada is ideal for studying LES.

LES is a meso-beta-scale system that is produced when cold and dry continental polar air advects over relatively warm lakes, generating turbulent moisture and heat fluxes into the lower planetary boundary layer (PBL). Thermal and moisture exchange, in addition to downwind surface frictional convergence, destabilises the PBL, inducing greater boundary layer convection and the development of cloud and precipitation along the leeward shores of lakes (Wiggin 1950; Eichenlaub 1970, 1979; Holroyd III 1971; Hozumi and Magono 1984; Pease et al. 1988; Leathers and Ellis 1993; Niziol et al. 1995; Ballentine et al. 1998; Kristovich and Laird 1998; Burnett et al. 2003; Notaro et al. 2013a, b; Campbell et al. 2016; Xiao et al. 2017). One main region of interest that warrants continued LES research, within the context of climate change, is the Canadian snowbelts of the Laurentian Great Lakes Basin (GLB).

The Laurentian Great Lakes are of prime research interest because they support Canada's economic, agricultural and industrial sectors (ECCC 2017). The occurrence of LES, however, can have destructive impacts on homes and pose commuting hazards to the 1.5 million people residing along the

✉ Janine A. Bajinath-Rodino
jabajna@uwaterloo.ca

¹ Department of Geography and Environmental Management and Interdisciplinary Centre on Climate Change, University of Waterloo, 200 University Avenue West, Waterloo, ON N2L 3G1, Canada

Canadian snowbelt of Lake Huron and 200,000 people along that of Lake Superior's (Norton and Bolsenga 1993; Kunkel et al. 2000; Burnett et al. 2003; Kristovich and Spinar 2005; Hartmann et al. 2013; NOAA GLERL 2017), thereby making the GLB an important region to study. Furthermore, continuous anthropogenic warming significantly influences the variability in temperature and precipitation (Albritton et al. 2001; Burnett et al. 2003), modifying the frequency, spatial and temporal distribution of heavy LES. High-impact weather events are important in adaptation studies, and many of these extreme events are better simulated in higher resolution modelling systems (Zadra et al. 2008).

There are limited validation studies evaluating the performance of high-resolution climate models to predict and delineate snowfall along the Canadian snowbelts of the Laurentian GLB. Of the few modelling LES studies, most employed relatively coarse global climate models (GCMs). For instance, Cohen and Allsopp (1988) used an $8^\circ \times 10^\circ$ spatial resolution and inferred the reduction of snowfall downwind of Lake Huron and Lake Ontario in response to a doubled CO_2 scenario. Similarly, Kunkel et al. (2002) used two coarse GCMs to investigate projected changes in the frequency of weather conditions favourable for the development of LES along the shores of Lake Erie during the late twentieth and twenty-first centuries. Their results are consistent with Cohen and Allsopp (1988), suggesting that LES downwind of Lake Erie will become less abundant. However, the relatively coarse resolution of GCMs makes it challenging for these studies to accurately resolve meso-beta-scale snowsqualls and snow bands, thus suggesting the need to employ higher resolution regional climate models (RCMs).

However, there is a lack in simulated historic LES studies using high spatial resolution RCMs (finer than 25 km resolution). Only a few studies have employed RCMs to assess historic and future LES projections. For example, Notaro et al. (2013a, b) used the 25-km Regional Climate Model Version 4 (RegCM4), with initial lateral boundary conditions obtained from the National Centers for Environmental Prediction, National Center for Atmospheric Research (NCEP, NCAR) reanalysis (Kalnay et al. 1996). The model was interactively coupled to the one-dimensional Hostetler Lake model to investigate historical (1976–2002) simulated snowfall across the GLB. The meso-beta-scale features of LES were well reproducible by the model. Simulations showed an abundance of LES downwind of Lake Ontario and Lake Erie in response to cold surges associated with an anticyclone in the central USA and a cyclone positioned over the northeastern USA. These RCM results were consistent with observational studies by Niziol (1987), Leathers and Ellis (1996) and Ballentine et al. (1998).

Additional studies include Vavrus et al. (2013) who also employed the 25-km resolution RegCM4 to simulate (1976–2002) ice cover concentrations over the Laurentian Great

Lakes. They observed negative trends in ice cover, attributable to warming in the twenty-first century, and suggest that changes towards more open water should favour the production of LES. This LES projection is in contrast with GCM ensemble predictions, under the special report emission scenarios (SRES) A1B greenhouse gas emission. The GCM ensemble projects fewer extreme cold-air outbreaks by 50 to 100% over the Northern Hemisphere, which could reduce the likelihood of LES development. These studies present contradicting projections of LES trends in response to climate change. The former suggests a potential future increase in LES, as ice cover decreases, while the latter suggests a decrease in LES due to fewer cold-air outbreaks. These opposing predictions highlight the need for LES model validation studies under contemporary climate conditions.

This paper examines the performance of a high-resolution 0.11° (ca. 12 km) Canadian Regional Climate Model version 5 (CRCM5) coupled to the one-dimensional Freshwater Lake model (FLake) (Mironov et al. 2010) to predict and delineate lake-induced precipitation events along the Canadian snowbelts of the Laurentian Great Lakes. CRCM5 is evaluated by first comparing historical (1995–2014) model simulations of snow water equivalent (SWE), winter precipitation, and LES predictor variables to that of datasets from Daymet Version 3 (Daymet), the North American Regional Reanalysis (NARR), or the National Oceanic and Atmospheric Administration (NOAA). Furthermore, seven selected and observed lake-induced precipitation events during high and low ice seasons for the months of December and January are compared to that of CRCM5's outputs to identify whether the model can capture the location, duration and precipitation accumulation of the events along Lake Superior's or Lake Huron's snowbelts. Identifying potential historical biases within the coupled high-resolution RCM is of critical information prior to using CRCM5 to predict future lake-induced precipitation scenarios.

2 Data and methodology

To evaluate the CRCM5's performance in predicting lake-induced precipitation, wintertime SWE and precipitation outputs were examined for the LES months of December and January (1995–2014). This time period was selected based on the availability of data. The lower time bound was limited by the availability of monthly lake surface temperature (LST) data, with records starting in January 1995. The upper bound was limited by CRCM5 data, ending in December 2014. SWE and precipitation from CRCM5 were statistically compared to those from the Daymet gridded interpolated dataset. Key LES predictor variables were also compared between CRCM5 and additional datasets in order to understand the performance of the CRCM5 in predicting lake-induced snowfall. The

predictor variables include 850 mb air temperature, LST and ice cover concentration. Furthermore, model validation was conducted on seven selected observed lake-induced events to determine whether the model could capture the timing, location and precipitation accumulation of these events.

2.1 Model description

2.1.1 Description of CRCM5

In this study, simulation outputs are produced from the latest version of CRCM, that is, Version 5. For several reasons, the CRCM5 was selected for this lake-induced investigation study. It has a relatively high, 0.11° (12 km), spatial resolution that is capable of resolving narrower meso-beta snowsqualls, not possible by coarser RCMs. All CRCM5 simulations, by default, use 56 vertical levels (Lucas-Picher et al. 2016). Ten of these levels are below 850 mb and are important for capturing mesoscale convective features. The lateral boundary conditions are driven by the European Reanalysis (ERA) Interim from 1979 onwards (Dee et al. 2011) on a grid mesh of 0.75° . The ERA Interim fields that force CRCM5 at the lateral boundaries include the horizontal wind components, temperature, specific humidity and surface pressure. These variables are available at 6-h intervals with a linear temporal interpolation that is used for providing the CRCM5 with data at every time step (Lucas-Picher et al. 2016). One-hour outputs of CRCM5 data are available and will be used later in this study when examining the seven lake-induced precipitation events.

The first version of CRCM was developed in 1991 at the Université du Québec à Montréal (UQAM). CRCM5 is based on the global numerical weather prediction model (GEM) of Environment and Climate Change Canada (ECCC), which employs the semi-Lagrangian transport and implicit marching scheme. It has a fully elastic non-hydrostatic formulation and uses a vertical coordinate based on hydrostatic pressure (Laprise 1992). In CRCM5, the usual GEM land surface scheme is replaced by the Canadian land surface scheme (CLASS) Version 3.4 (Verseghy 2009) and then later by Version 3.5 that allows a mosaic representation of land surface types. While in numerical weather prediction (NWP) applications of GEM, LST and ice fraction are prescribed using the climatological Atmospheric Model Intercomparison Project (AMIP II), these prescriptions are inappropriate for climate change projections. Future climate projections require an interactive lake parameterisation scheme (Martynov et al. 2012) so that accurate estimates of lake processes, including ice cover extent, can be used for improved predictions in climate studies (Scott et al. 2012). Thus, Martynov et al. (2012) tested and compared model simulations of CRCM5 interactively coupled to lake models. The CRCM5 has been coupled to the one-dimensional FLake model (Mironov et al. 2010) and

separately to the Hostetler model (HL) (Hostetler and Bartlein 1990; Hostetler 1991, 1995; Hostetler et al. 1993; Bates et al. 1993, 1995). The CRCM5 simulations coupled to the two lake models were provided by the UQAM–Canadian Network for Regional Climate and Weather Processes (CNRCWP) working group.

2.1.2 Description of FLake

The current study employs the CRCM5 model run coupled to the interactive FLake model. FLake was chosen for this study because Martynov et al. (2012) showed that FLake outperformed other one-dimensional lake model predictions over the GLB. FLake is a one-dimensional column model with a two-layered time varying temperature profile (Mironov 2008; Mallard et al. 2014). The two-layered water temperature profile has a mixed layer at the surface and a thermocline extending from the mixed layer to the bottom of the lake. A system of prognostic ordinary differential equations is solved to obtain the thermocline shape coefficient, temperature of active sediment layer, ice and snow temperatures, surface and lower level water temperatures and mixed layer depth.

The mixed layer depth equation includes convective entrainment, wind-driven mixing and volumetric solar radiation absorption. The two-layer water temperature limits the lake model's performance for deep lakes because it does not resolve the hypolimnion layer between the thermocline and the lake bottom. A solution is to simulate a virtual bottom that is assigned between 40 and 60 m (Martynov et al. 2012; Mallard et al. 2014). In this CRCM5–FLake simulation, a maximum lake depth of 60 m is assigned for all lakes with depths greater than 60 m, such as the Laurentian Great Lakes (Katja Winger, 2017, personal communication). Temperature changes in the deep abyssal zone is not appreciable; thus, assigning a false bottom approximation produces satisfactory results (Gula and Peltier 2012).

Furthermore, a snow module is included in FLake but is advised against using by the model developers until further improvement. However, a correction of the ice albedo, which takes into account the influence of snow albedo, is applied and is usually assigned a value between 0.2 and 0.3. Finally, FLake does not allow partial ice cover for each grid cell (Martynov et al. 2012). This could be a potential limitation in the analysis and will be elaborated on in Section 3. FLake is well tested because it has been coupled to different NWPs and RCMs, such as studies conducted by Kourzeneva et al. (2008), Martynov et al. (2008), Mironov et al. (2010) and Samuelsson et al. (2010), and has further been evaluated against other lake models, including studies by Martynov et al. (2010), Kheyrollah Pour et al. (2012), Semmler et al. (2012) and Mallard et al. (2014).

2.2 Description of datasets used for evaluation

The CRCM5 modelled outputs were compared against several other datasets. These datasets comprise Daymet, NARR, NOAA Great Lakes Ice Atlas, NOAA Coast Watch and ECCC's historical data archives.

2.2.1 Daymet

Gridded interpolated SWE and precipitation data were acquired from the Oak Ridge National Laboratory Daymet product. The Daymet product is employed because it offers a high spatial gridded resolution that is ideal for delineating localised precipitation bands indicative of lake effect snowfall events during the winter months. In this study, the Daymet data was up-scaled from its native grid to the coarser CRCM5, 0.11°, grid using bi-linear interpolation. This conversion enables spatial comparison between the gridded datasets.

Daymet interpolates and extrapolates data to produce 1-km resolution weather parameters over larger regions (Thornton et al. 1997, 2000). Daymet requires input from models such as a digital elevation model and uses ground-based observations from weather stations. The digital elevation model is a subset of the National Aeronautics and Space Administration's (NASA) Shuttle Radar Topography Mission 2.1 (SRTM). The in situ weather observations are acquired from the Global Historical Climatology Network (GHCN) under the NOAA (Menne et al. 2012). The interpolation method is based on the spatial convolution of a truncated Gaussian weighting filter with sets of station locations. The dataset was developed by the Environmental Sciences Division at the Oak Ridge National Laboratory (Thornton et al. 1997, 2000). A detailed description of this dataset can be found at <http://daymet.ornl.gov>.

It is acknowledged that Daymet gridded data are interpolated from weather station sites and are prone to uncertainties. Thus, annual cross-validation statistics for Daymet's (Version 3) were generated by station-based daily observations and predictions for 2° × 2° tiles over North America (Thornton et al. 2016). Each tile provides period-of-record mean absolute error (MAE) and bias statistics for input weather observations of maximum and minimum temperature and precipitation for each year, 1980–2016. Further details on Daymet's data validation can be found at https://daac.ornl.gov/DAYMET/guides/Daymet_V3_CrossVal.html#revisions.

Furthermore, SWE estimates are executed by employing a single calendar year of primary surface inputs, including daily maximum and minimum temperature and daily total precipitation. Because higher latitude snow packs are normally underway at the beginning of the calendar year, the SWE algorithm uses data from a single calendar year to make a 2-year sequence of temperature and precipitation that predicts the evolution of the snowpack. This provides an estimate of the

snowpack at day 365 as an initial condition for the January 1st time step. However, because this approach ignores the dependence of January 1st snowpack on the preceding calendar year's temperature and precipitation conditions, it may generate potential biases in mid-season snowpack that can propagate to biases in late season timing of snowmelt. Additional information can be found at: https://daac.ornl.gov/DAYMET/guides/Daymet_V3_CFMosaics.html.

These limitations were considered when evaluating the performance of the CRCM5 with the Daymet data. This is why additional comparisons of snowfall were conducted by using Doppler radar data, discussed later. Although other SWE products are available, either the spatial resolution is too coarse to delineate snowfall within the relatively narrow snowbelt regions or the temporal coverage is too short for the purposes of this study, and examples include Canadian Sea Ice Evolution (CanSISE) observation Version 2 and Snow Data Assimilation System (SNODAS) data product Version 2, respectively. Thus, for the purposes of this study, SWE generated by Daymet was the best option.

2.2.2 NARR

The NARR dataset is used for providing high-frequency and dynamically consistent surface–atmosphere gridded reanalysis variables, including 850 mb air temperature. NARR assimilates meteorological observations to produce land and surface model updates. Three-hourly observations are collected and assimilated using a three-dimensional variation (3D-Var) approach with a model integration period of 3 h, for which a short-range forecast is produced. This result is then fed, as the initial condition, into the next cycle, where the system repeats itself with updated observational data (Mesinger 2006). Furthermore, NARR comprises the NCEP Eta model at 32 km resolution and 45 vertical layers, data assimilation schemes, the Noah land-surface model and lateral boundary forcing from the NCEP-Department of Energy (DOE) Global reanalysis. NARR is a reliable reanalysis dataset for representing LES predictor variables. It has been validated with both surface stations and sounding measurements and is proven as a trustworthy source for atmospheric reanalysis data in numerous North American validation climate studies (Mesinger 2006; Lo et al. 2008; Gula and Peltier 2012). NARR is produced by the NOAA NCEP in Boulder, CO, USA, and is accessible through the NOAA website <http://www.esrl.noaa.gov/psd/>.

2.2.3 NOAA ice atlas and coast watch

Two data sources were used to provide the most comprehensive ice cover data. The electronic atlas of Great Lakes ice cover provided data for the years 1973 to 2005 and is available by NOAA Great Lakes Environmental Research Laboratory

(GLERL). NOAA provides composite ice charts, which are a blend of observations from ships, shore stations, aircraft and satellites to estimate ice cover data for the entire Great Lakes. The ice charts were digitised and made available at <https://www.glerl.noaa.gov/data/ice/atlas/index.html>.

Also, NOAA GLERL Coast Watch provides observed lake-wide averaged monthly mean LSTs and ice cover from 2008 to present. Coast Watch is a NOAA programme that delivers environmental products and data in near-real time observations of the Great Lakes using three main satellite observations. NOAA's Advanced Very High Resolution Radiometer satellite (AVHRR) provides 33 enhanced digital images of satellite-derived surface temperature, visible and near-infrared reflectance, brightness temperature, cloud masks and satellite solar zenith angle data. The Geostationary Operation Environment Satellite (GOES) provides near-infrared and water vapour data. Finally, the Moderate Resolution Imaging Spectroradiometer (MODIS) satellite provides true colour 250 m resolution imagery of each Great Lake. Furthermore, in situ measurements and modelled data, such as marine meteorological observations, buoy from NOAA's National Ocean Service and Great Lakes Surface Environmental Analysis (GLSEA) composite charts, are acquired, produced, stored and made available to the Great Lakes Coast Watch users. Further details are available at <https://coastwatch.glerl.noaa.gov/overview/cw-overview.html> (Wang et al. 2012, 2017).

Because the observed ice cover data was acquired from the electronic atlas of Great Lakes from 1973 to 2005 and then from NOAA GLERL Coast Watch from 2008 to present, the observational cold season of 2005/2006 to 2007/2008 are not available. However, this does not pose an issue, as the study focuses on in the inter-annual variability as opposed to climatic trends. Furthermore, the focus was to capture years of high and low ice cover concentrations and LST to determine whether the model was able to reproduce some of these annual observations. It is also acknowledged that Canadian Ice Service (CIS) has a complete temporal coverage of monthly total accumulated ice cover. However, CRCM5 data comprises monthly mean ice cover. Therefore, to make ice cover

comparisons consistent between CRCM5 and observations, the NOAA GLERL datasets were used because they also provide monthly mean ice cover.

2.2.4 Radar and weather station data from ECCC

Specific lake-induced precipitation events were analysed by identifying observational data from ECCC's historical archive data, found at the National Climate Data and Information Archive, <http://climate.weather.gc.ca>. Historical ground-based weather observation stations and radar imagery were used to identify the location, duration and precipitation accumulation of observed lake-induced events that were compared against model predictions. The weather observation stations provide the daily total precipitation in millimetres for the specified locations observed. The daily total precipitation acquired from ECCC is defined as the sum of total rainfall and water equivalent of total snowfall in millimetres observed at the location (ECCC 2018). In addition to the weather stations, a network of ground-based weather radars, which have a detection range of 250 km radius and a Doppler range of 120 km, was also used to determine the events. For cities analysed along Lake Superior's snowbelt, the Montreal River (near Sault Ste. Marie) radar was utilised. For cities along Lake Huron's snowbelt, either King City (near Toronto) or Exeter (near London Ontario) radar was employed. The two ECCC sources, which are the ground observation stations and the radar networks, were applied in unison for identifying lake-induced precipitation in order to reduce common radar analysis errors such as overshooting beams and virga detection. Table 1 lists the cities and their associated weather station coordinates used for acquiring observed precipitation accumulations, snowbelts, observation radars and grid cells for obtaining the predicted precipitation accumulation.

2.3 Assessment of model performance

The study regions of interest focused on the Canadian snowbelts of Lakes Superior and Huron. In order to delineate whether the model captures wintertime lake-induced

Table 1 Description of the cities and their associated weather station coordinates, snowbelt, radar and modelled grid cell coordinates

City	Weather station coordinates	Snowbelt	Radar	CRCM5 grid cell location
Barrie	44.39, - 79.74	Huron	King City	$X = 357$ $Y = 281$
Sault Ste. Marie	46.39, - 84.5	Superior	Montreal River	$X = 357$ $Y = 281$
Wawa	47.9, - 84.78	Superior	Montreal River	$X = 377$ $Y = 308$
Warton	44.75, - 81.11	Huron	Exeter	$X = 385$ $Y = 175$

precipitation for the two snowbelt regions, gridded SWE and total precipitation were analysed for the entire Laurentian GLB within the coordinates of 94 W, 74 W, 40 N and 50 N. SWE and precipitation were analysed by computing the monthly mean SWE and monthly precipitation totals for December and January (separately) for each of the 20 years (1995–2014). Statistical indices were employed followed by analyses of selected lake-induced events.

2.3.1 Statistical evaluations

Three statistical indices of model performance were employed over the 20-year period and include the 20-year SWE and precipitation averages for both CRCM5 and Daymet. The root mean square difference (RMSD) and the mean bias difference (MBD) were computed. The 20-year averages were calculated for the monthly mean SWE and total precipitation for December and separately for January.

The RMSD was also computed for December and January and indicates the magnitude of the average difference (Eq. 1). Additionally, RMSD was calculated for each grid cell within the GLB. Similarly, MBD is analysed and given in Eq. 2. MBD describes the direction of the error bias; for example, a negative bias suggests that the model simulation underestimates the prediction when compared to the observed output (Chow et al. 2006). In Eqs. 1 and 2, pr represents the predicted value, o represents the observed value and n is the number of data values used.

$$\text{RMSD} = \sqrt{\frac{\sum_{n=1}^{20} (pr-o)^2}{n}} \quad (1)$$

$$\text{MBD} = \frac{\sum_{n=1}^{20} (pr-o)}{n} \quad (2)$$

In order to understand the predictive performance of the model in capturing SWE and wintertime precipitation, 20-year time series were analysed for LES predictor variables followed by an examination of their RMSD and MBD. Monthly means of each predictor variable were computed separately for December and January for each year between 1995 and 2014. Table 2 shows the list of variables along with their temporal range and sources, which will be discussed in the results section.

2.3.2 Assessment of lake-induced precipitation events

Further model assessments on predicting lake-induced snowfall were conducted by determining whether the model could capture the timing, location and precipitation accumulation of

Table 2 List of datasets with associated variables, sources and temporal availability used in this study

Dataset	Temporal availability	Variables	Source
CRCM5	January 1980–December 2014	<ul style="list-style-type: none"> • SWE • Precipitation • Mixed layer depth (LST) • Ice cover • 850 mb air temperature 	Université du Québec à Montréal
Daymet Version 3	January 1980–December 2014	<ul style="list-style-type: none"> • SWE 	https://daac.ornl.gov/DAYMET/guides/Daymet_V3_CFMosaics.html#revisions
NARR	January 1979–December 2014	<ul style="list-style-type: none"> • Precipitation • 850 mb air temperature 	https://www.esrl.noaa.gov/psd/data/gridded/data.narr.pressure.html
NOAA Coast Watch	November 1994–December 2014	<ul style="list-style-type: none"> • LST 	https://coastwatch.glerl.noaa.gov
NOAA Coast Watch	December 2008–March 2014	<ul style="list-style-type: none"> • Ice cover concentration 	https://coastwatch.glerl.noaa.gov
NOAA Great Lakes Ice Atlas	December 1973–December 2005	<ul style="list-style-type: none"> • Ice cover concentration 	https://www.glerl.noaa.gov/data/ice/atlas/daily_ice_cover/daily_averages/dailyave.html https://www.glerl.noaa.gov/pubs/tech_reports/glel-135/Appendix2/DailyLakeAverages/
Historical Weather Radar	2007–2014	<ul style="list-style-type: none"> • Snowfall rate 	http://climate.weather.gc.ca
Historical Weather Station Observations	2011–2014	<ul style="list-style-type: none"> • Precipitation accumulation 	http://climate.weather.gc.ca/historical_data/search_historic_data_e.html

selected events for Lake Superior and Lake Huron snowbelt regions. The selected events were narrowed down by snowfall that either occurred along Lakes Superior or Huron's snowbelt, during the LES months of December or January and during years of either low or high ice season. This is because ice cover is a determining variable in producing LES. In total, seven events were analysed using four cities, two that represent the Superior snowbelt, Wawa and Sault Ste. Marie, and two that represent the Huron snowbelt, Barrie and Wiarton. Observations were limited to four cities and two LES seasons in order to reduce additional influences in LES predictions, such as microclimate influences, differences in station data gathering techniques and climatic seasonal variations. These restrictions maintained a sense of consistency when comparing the model's performance in the different events.

Lake-induced precipitation events were determined when parallel snowsquall lines were observed from radar images along the leeward shores of Lakes Superior and Lake Huron and only extended to approximately 100 km inland. If widespread precipitation was noticed farther inland, this would not be considered a lake effect event. However, if localised squall lines developed after widespread precipitation moved through the region, this was an indication of lake-enhanced precipitation event.

When available, extreme lake-induced snowfall events were selected for this analysis. Extreme daily precipitation accumulations were retrieved, providing that observed snowfall were ≥ 15 cm/day (Bajinath-Rodino and Duguay 2018), or

if the equivalent liquid amount of 10 mm/day was recorded. The 10-mm liquid equivalent amount is determined by assuming that across the GLB, from December through February, the snow liquid ratio (SLR) is approximately 15:1 in. (Baxter et al. 2005), or 38.1 cm of snow to 25.4 mm of water; thus, a 15-cm snowfall would equal 10 mm of liquid water equivalent.

Apart from precipitation accumulation, timing was also documented by recording how long an event occurred in a particular location. The predicted precipitation accumulation amounts were best captured by determining the grid cell where the observed city was located and aggregating its hourly precipitation value within the day it occurred, starting at 00:00 and ending at 23:00. The CRCM5 hourly snowfall prediction of the duration, location and precipitation accumulation was compared against the observed events and analysed in Section 3.

3 Results and discussion

3.1 SWE and precipitation

Model evaluation was first carried out by comparing SWE outputs. Figure 1a, b shows the averaged 1995 to 2014 December SWE totals for CRCM5 and Daymet, respectively. The spatial results indicate a predominant discrepancy in simulated SWE along the Canadian leeward shores

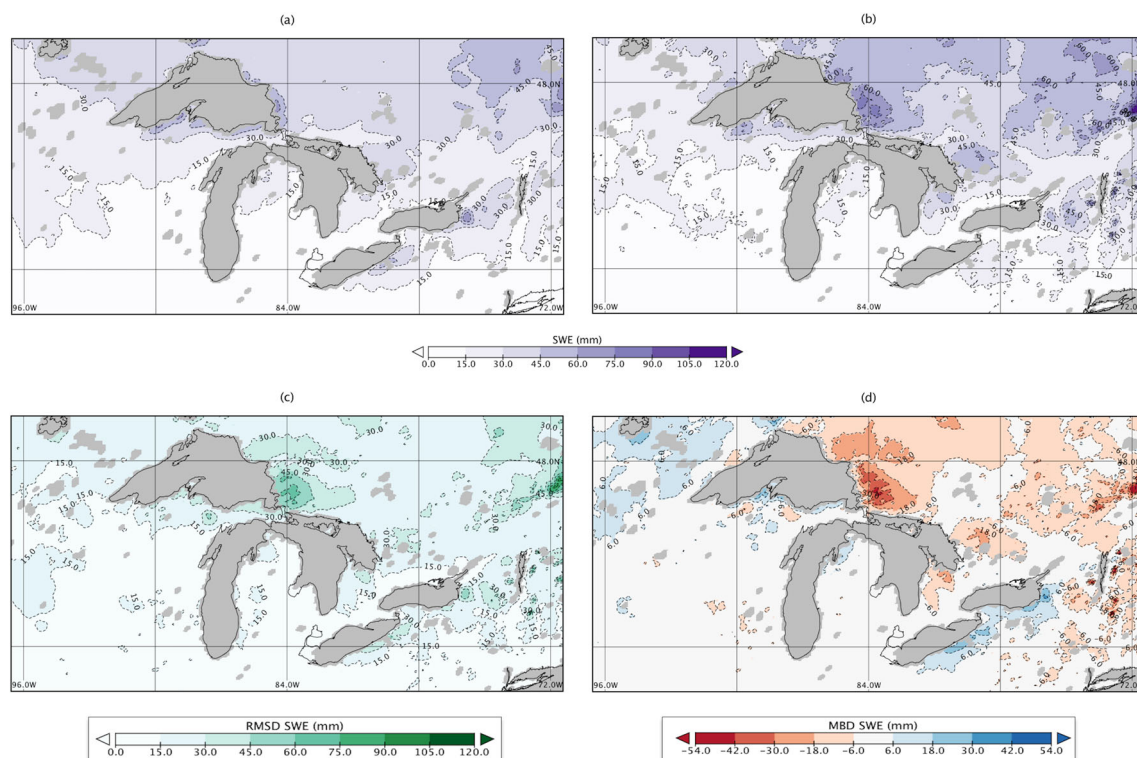


Fig. 1 December mean SWE averaged over 1995 to 2014 for **a** CRCM5, **b** Daymet, **c** RMSD and **d** MBD

of Lakes Superior and Huron. Higher Daymet SWE averages, of approximately 60 mm, are seen along Lake Superior's snowbelt, whereas CRCM5 values closer to 40 mm are predicted. Heavier Daymet SWE averages of 40 mm are also seen along Lake Huron's snowbelt, in contrast to values of approximately 20 mm shown in the CRCM5. RMSD values are upwards of 30 mm predominantly along both snowbelts (Fig. 1c). MBD indicates a negative bias upwards of 20 mm along both snowbelts, indicating that the model is under-predicting SWE along the Canadian leeward shores (Fig. 1d).

Similarly, Fig. 2 presents the averaged 1995 to 2014 January SWE totals. Unlike the CRCM5 prediction in Fig. 2a, higher amounts of averaged SWE, upwards of 100 mm, are shown for Daymet (Fig. 2b) along the leeward shores of the two snowbelts. The RMSD value indicates values closer to 60 mm along both snowbelts (Fig. 2c) and a higher SWE MBD of 50 mm (Fig. 2d). Thus, both LES months show a predominant under-estimation of simulated SWE along both Canadian snowbelts.

The resultant spatial discrepancy along the snowbelts suggests that lake effect snowfall and its processes may not be accurately predicted in the coupled Flake-CRCM5 simulation. Experiments conducted by Lucas-Picher et al. (2016) suggest that additional information can be extracted from CRCM5 when downscaling from a resolution of 0.44 to 0.11. The higher resolution CRCM5 improved

the orography and allowed for higher accuracy of small-scale lake effect snow processes along the snowbelts. Despite the added value of the higher resolution CRCM5, results of Figs. 1 and 2 indicate that there is an under-estimation of simulated SWE, predominantly along the Canadian leeward shores of Lakes Superior and Huron. However, SWE is subject to snow metamorphosis processes, such as melting, re-freezing, densification and re-distribution from surface winds. Therefore, to determine whether the model can accurately predict lake effect snowfall events, wintertime precipitation is also analysed.

The averaged 1995 to 2014 December precipitation totals for CRCM5 and Daymet outputs are shown in panels a and b of Fig. 3, respectively. Although the CRCM5 captures higher amounts of precipitation along the snowbelts, relative to farther inland (Fig. 3a), the location and amount are not accurately predicted. The RMSD shows values of approximately 40 mm along both snowbelts (Fig. 3c). The MBD also indicates negative biases of approximately 30 mm along the southeastern shores of Lake Superior and 10 mm along Lake Huron's leeward shores (Fig. 3d).

Furthermore, the January precipitation totals are computed and are presented in Fig. 4. Relative to precipitation in December, results show less amounts of precipitation in January along Lake Superior's snowbelt (Fig. 4a, b), respectively. The RMSD is relatively low along Lake Superior's snowbelt (Fig. 4c) compared to a higher RMSD values of

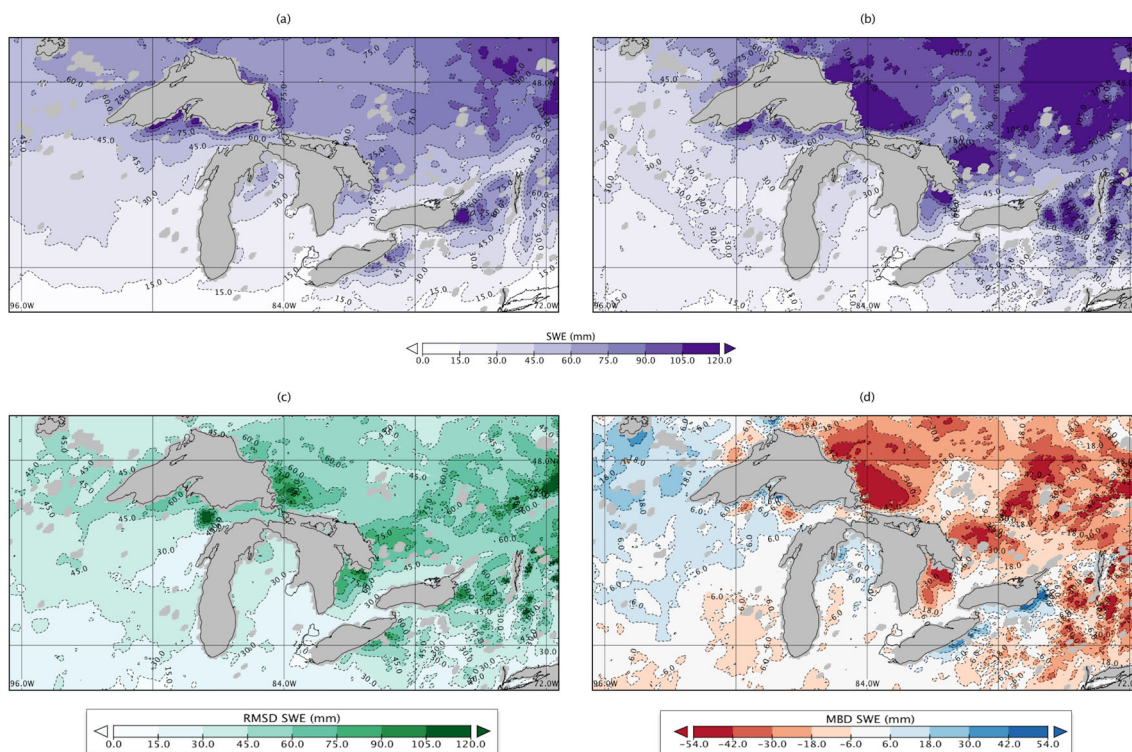


Fig. 2 January mean SWE averaged over 1995 to 2014 for **a** CRCM5, **b** Daymet, **c** RMSD and **d** MBD

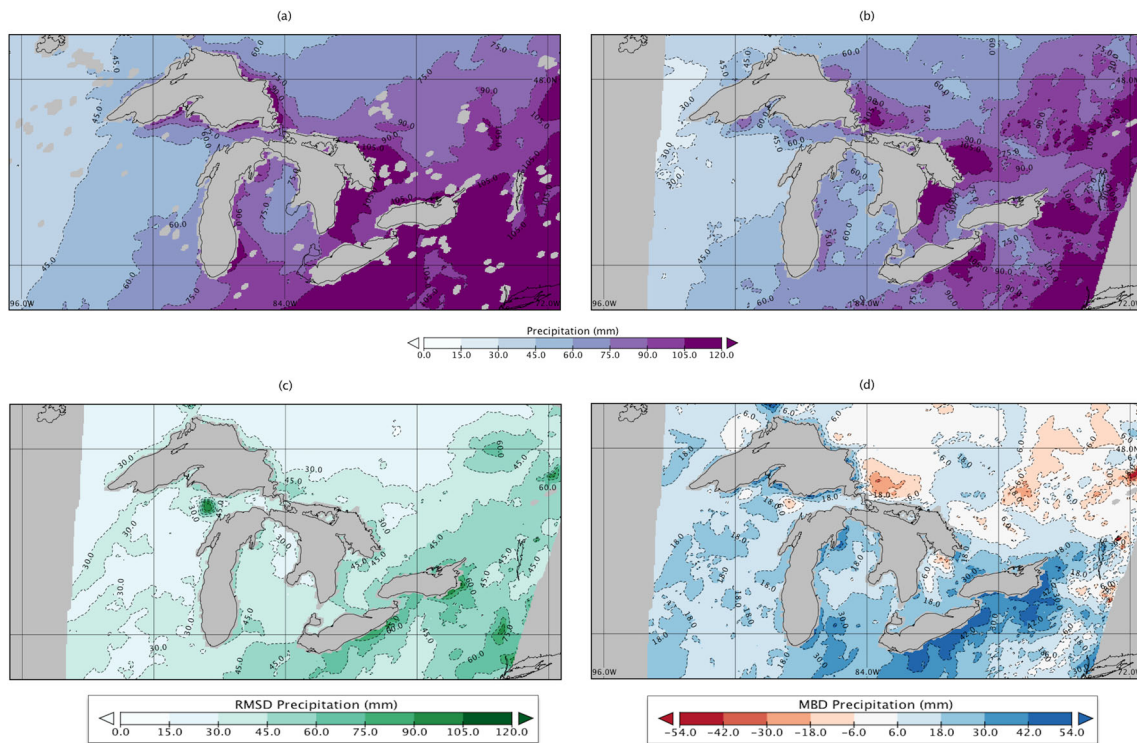


Fig. 3 December total precipitation averaged over 1995 to 2014 for **a** CRCM5, **b** Daymet, **c** RMSD and **d** MBD

40 mm for Lake Huron’s snowbelt. Figure 4d shows the MBD values, which are predominantly negatively biased along the leeward shores of Lake Huron, straddling the north and south shores of Georgian Bay.

Similar to the SWE results, precipitation evaluation indicates that the CRCM5 also under-estimates wintertime precipitation. The results, showing the location and accumulation discrepancy in wintertime precipitation along the Canadian

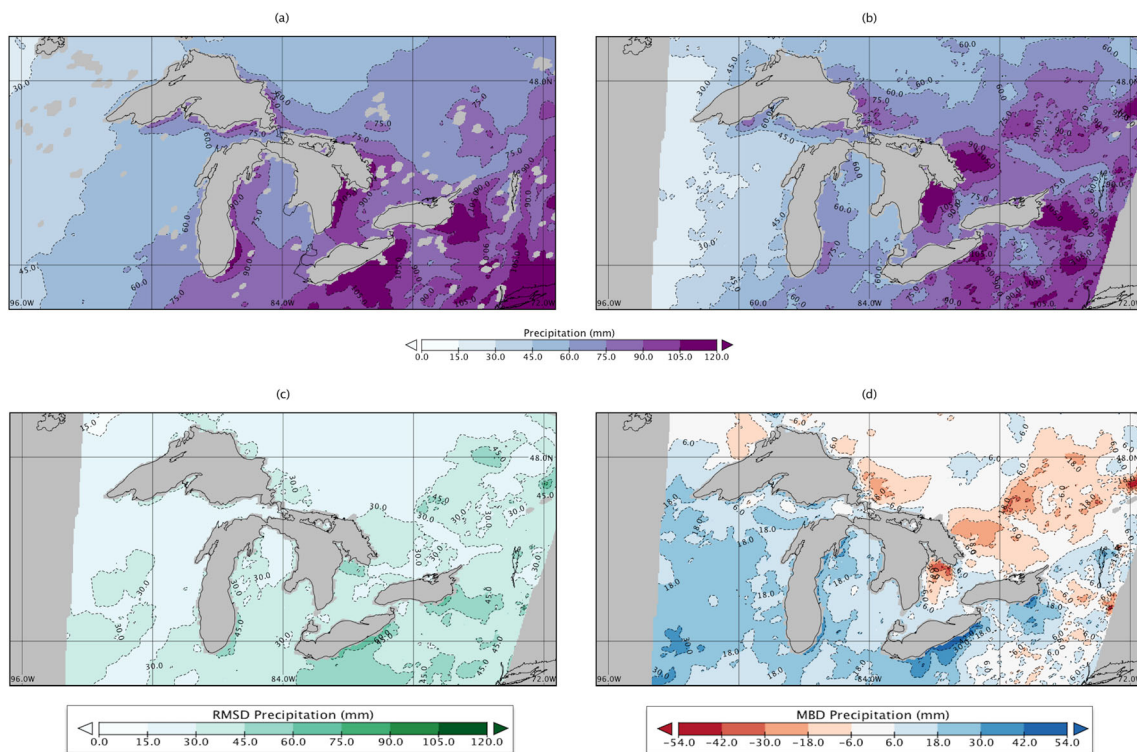


Fig. 4 January total precipitation averaged over 1995 to 2014 for **a** CRCM5, **b** Daymet, **c** RMSD and **d** MBD

leeward shores of Lake Superior and Lake Huron, further reinforce that the CRCM5 may not fully capture lake effect snowfall and its surface–atmosphere processes.

3.2 Lake-induced precipitation events

To further evaluate the model's predictive performance in capturing lake-induced snowfall, seven separate events were documented and analysed. Events 1 through 4 were taken during the high ice season of 2013–2014, during the months of December or January, and located on either the Superior or Huron snowbelt. Events 5a and 5b through event 7 were

similarly examined, but for the low ice season of 2011–2012. Figure 5 shows a timestamp of each simulated and observed event, 1 through 7.

The first event was documented for Wawa on January 28, 2014. Event 1 was observed as an extreme lake-enhanced snowfall event for the Lake Superior snowbelt. The synoptic system moved through the region prior to 00:00 January 28 and dissipated around 18:00 on January 29 with snowsqualls lasting approximately 42 h. Observed squall bands moved from south, along Superior's snowbelt, to north, bringing 10.4 mm of precipitation to Wawa. The model simulation also predicted that event 1 started prior to January 28 00:00 and

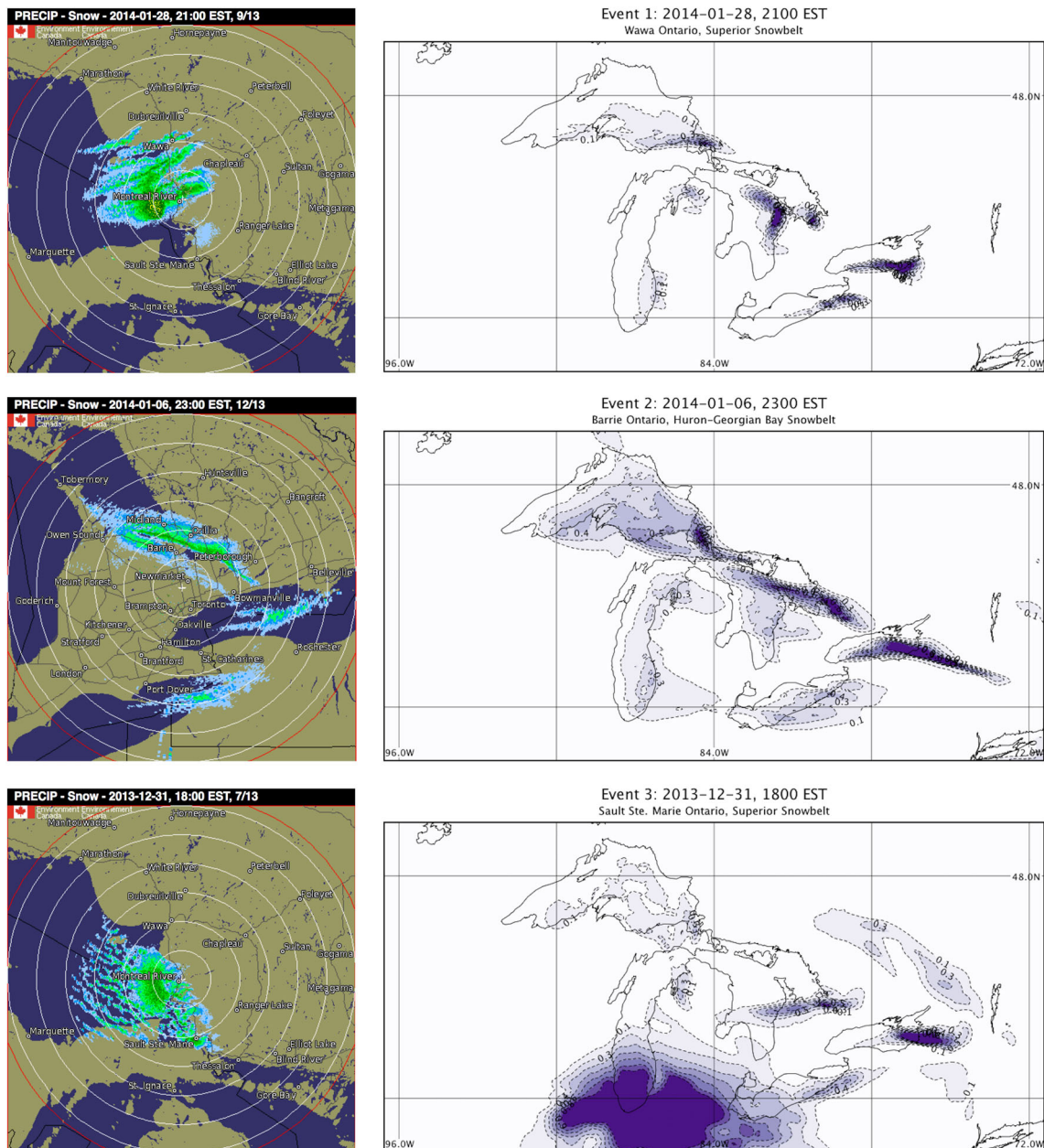


Fig. 5 Lake-induced events 1 through 7 with radar observations (left) and CRCM5 predictions (right)

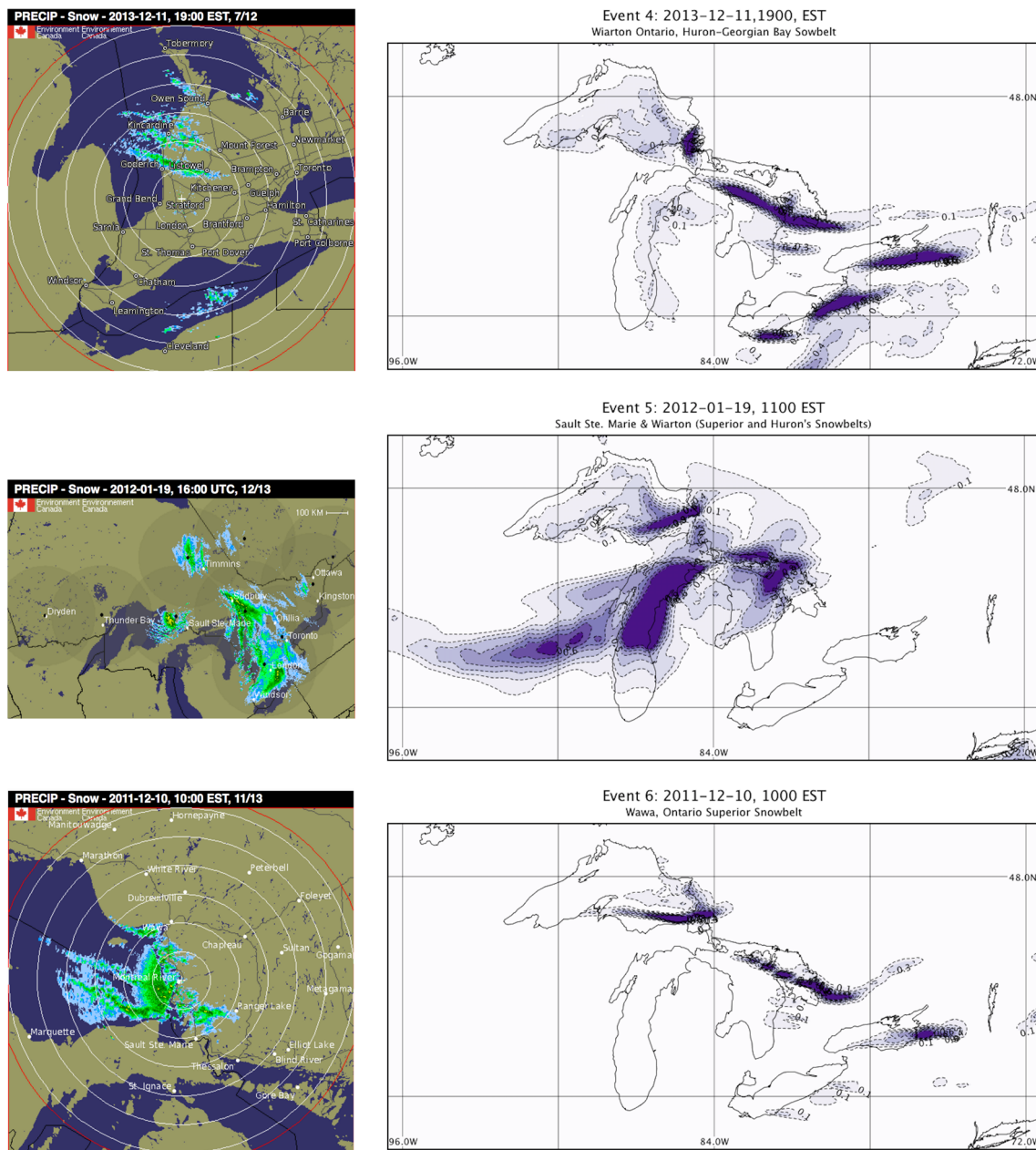


Fig. 5 (continued)

dissipated approximately 45 h later. The simulated hourly aggregated daily precipitation, taken from January 28 00:00 to January 28 23:00, only summed 0.3 mm within the model’s grid cell. The model’s timing of the event is similar to that of observations; however, the accumulation of precipitation is grossly under-estimated. This could be attributed to the wind direction of the predicted snowsqualls. For example, while the observations recorded winds from a west–southwest direction, which advected squalls northeastward towards Wawa, the predicted squalls showed a southwesterly flow, advecting precipitation farther south away from Wawa. Figure 5, event 1, shows the observation and simulation of the event,

respectively, for January 28, 2014, at 21:00 EST, and show the different directions of the squall band locations as they move onshore of Lake Superior’s snowbelt. In conclusion, the model under-estimates the daily precipitation accumulation for this event; it also misses the location of the squall bands but produces a similar onset of the event.

The second event was recorded for Barrie along Lake Huron’s snowbelt on January 6, 2014. This event was observed as an extreme lake-enhanced snowfall event. A synoptic scale system moved through the GLB from January 5 into the early morning of January 6 and snowsqualls developed behind the synoptic system, ushering snowsqualls to Barrie

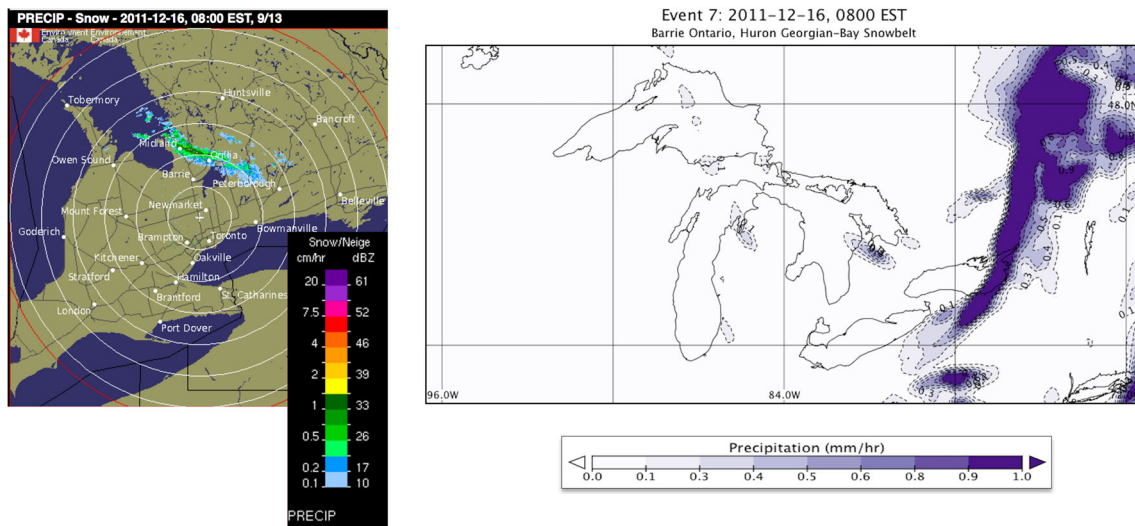


Fig. 5 (continued)

off of Georgian Bay with a northwesterly flow. The squalls started by 07:00 January 6 to approximately 07:00 on January 8 with a duration of about 48 h. The observed daily precipitation in Barrie on January 6 was 19.0 mm, making this an extreme lake-induced snowfall event. In contrast, the model recorded no precipitation for Barrie on this day and did not capture the observed extreme event for this location. Nevertheless, the model was able to capture the trajectory and timing of the synoptic system that moved through the GLB, followed later by squalls. The model kept lingering precipitation bands in the Huron snowbelt region, while the radar shows these bands moving farther north as the wind profile switches to a southeasterly flow. Figure 5, event 2, shows the observed and simulated event respectively for January 6, 2014, at 23:00 EST. In conclusion, the daily accumulation associated with this extreme event was not captured by the model, but the timing and the general vicinity of the squall lines moving through the snowbelt were similar to that of observations.

The third event was recorded for Sault Ste. Marie, along Lake Superior's snowbelt on December 31, 2013. This observed extreme event was suggested to form from a weak Alberta Clipper that moved through the GLB from 00:00 December 31, 2013, to 09:00 January 1, 2014, bringing 13.8 mm of precipitation to Sault Ste. Marie. However, the model prediction of only 0.6 mm was recorded. Figure 5, event 3, shows the timestamp of this event on December 31, 2013, at 18:00 EST. The squall lines in the model are visibly difficult to delineate for the Sault Ste. Marie region. Despite the under-prediction in the daily precipitation accumulation, the model accurately predicted the onset, duration and the general location of the squalls.

The fourth event was observed at Wiarton along Lake Huron's snowbelt on December 11, 2013, and was considered

a pure lake effect event. The radar shows persistent lake effect squalls moving through Wiarton and then advecting southward away from the city. Snowfall started prior to 00:00 December 11, 2013, and ended at approximately 08:00 on December 12. It brought 8.1 mm of precipitation to the city. The model, however, predicted only 2.5 mm for that day. The predicted onset time was similar to that of the observed, except the model had squalls lingering until 21:00 December 13. The locations of the squalls were within the general snowbelt region as can be seen by Fig. 5, event 4, with the timestamp of December 11, 2013, at 19:00 EST. Overall, only the location of this event was well captured. The duration was over-predicted and the daily accumulation was under-predicted.

Event 5 was a lake-enhanced system that affected both Lakes Superior and Huron's snowbelts on January 19, 2012. Event 5a was analysed for Sault Ste. Marie and the Lake Superior's snowbelt, while event 5b was analysed for Wiarton and corresponds to Lake Huron's snowbelt. A synoptic system moved through the GLB overnight into the morning of January 19 and behind it was lake-enhanced squalls that developed around 11:00 towards Sault Ste. Marie and persisted into the morning of January 20. The cold front associated with this system then moved through Southern Ontario, bringing squalls to Lake Huron's snowbelt and the city of Wiarton. The timing of the system moving through Southern Ontario was delayed in the model and did not appear until later in the evening. Figure 5, event 5, shows the observed snowfall over Southern Ontario at 11:00 EST, while the model shows the precipitation still farther to the west of Southern Ontario at this time. Observed daily precipitation for Sault Ste. Marie, along Lake Superior's snowbelt, was 9.2 mm, but the model only predicted 2.7 mm. Furthermore, Wiarton's observed precipitation measurements, along Lake Huron's snowbelt, was 8.0 mm; however, the model only

predicted 4.7 mm. In conclusion, the model under-estimates the accumulated daily precipitation associated with this lake-enhanced system. The onset of the system is also delayed in the model; however, the general locations of the squalls are accurate.

The sixth event was observed as pure LES over Wawa for the Superior's snowbelt on December 10, 2011. The observed event started the evening of December 8 and ended the morning of December 10, bringing 3.6 mm of precipitation to the city. The model predicted earlier development of the squalls, starting overnight and into the early morning of December 8 and persisting until the night of December 10. The model predicted 4.9 mm of daily precipitation for December 10. In comparison to all the other selected events, this is the only event for which the model over-predicted the accumulation. The model also over-estimated the duration of this event but accurately captured the location of the observed squalls (Fig. 5), event 6, with timestamp of December 10, 2011, at 10:00 EST.

Finally, event 7 was a lake-enhanced snowfall event for Barrie along Lake Huron's snowbelt on December 16, 2011. A synoptic system moved over the GLB on December 15, and behind this system, snowsqualls developed over Georgian Bay. Squalls started in the early morning of December 16 and persisted until noon of December 17, producing 5.0 mm of precipitation. The model's estimated onset and duration of the event were accurately depicted, but it did not record any daily precipitation accumulation for Barrie on December 16. However, the model was able to capture the previous day precipitation accumulation for a larger synoptic system that moved through the region. The squall locations in the model are farther south towards Owen Sound and the squalls are short lived (Fig. 5), event 7, with a timestamp of December 16, 2011, at 08:00 EST.

Overall, these event analyses suggest that the model seems to accurately predict the timing and, to an extent, the location of the snowsqualls, but drastically under-estimates the daily precipitation associated with the lake-induced events. The model mostly captures the onset of snowsqualls and synoptic systems moving through the region. However, the model seems to prolong the duration of the event, extending the duration of the overall event longer than what was observed.

The model captures the general locations of squall lines moving towards the observed snowbelts. However, specific localised squalls are difficult to delineate by the model, such as squalls that occurred in Barrie, along Lake Huron's snowbelt, or Wawa, along Lake Superior's snowbelt. This could be that the 0.11° resolution of the model was too coarse to represent the highly localised squall lines associated with some of these LES bands. Perhaps higher resolution models, at resolutions of only 2 km, would better capture these highly localised bands since squall lines can be as narrow as 1–2 km. Furthermore, the model consistently under-predicts

precipitation accumulation, despite the month of the LES season, or the ice season, with the exception of one event. These results are in agreement with the previous results (recall Figs. 3 and 4) that suggest that precipitation is significantly under-predicted along the snowbelt regions of both Lakes Superior and Huron. Thus, the reasons for the predominant negative bias in lake-induced precipitation accumulations are explored by examining key LES predictor variables.

3.3 Atmospheric predictor variables

Key predictor variables, as suggested in previous literature, including Niziol et al. (1995), Cosgrove et al. (1996), Hamilton et al. (2006), Hartmann et al. (2013), Notaro et al. (2013a, b), Bajinath-Rodino et al. (2018) and Bajinath-Rodino and Duguay (2018), are 850 mb air temperature, LSTs (Wang et al. 2018) and ice cover concentration. Temperature plays a multifaceted role in the development of LES by influencing precipitation type and vertical instability. Lake effect precipitation will usually fall as a solid state when temperatures at the 850-mb level are below freezing. The vertical temperature gradient (VTG), which is the difference between the LST and 850 mb temperature, is an indicator of instability in the (PBL). In meteorology, a VTG greater than 13°C is a general indicator of an unstable lapse rate, which will induce moisture and energy fluxes into the lower PBL, inducing convection (Holroyd III 1971; Niziol 1987; Theeuwes et al. 2010; Hartmann et al. 2013). Thus, the 850-mb air temperature is an important feature that influences LES and is, therefore, warranted in this study.

In this paper, the CRCM5 and NARR outputs of 850 mb air temperature are represented on their native grids. This is because the NARR grid has a relatively coarse 32-km resolution and the CRCM5 would have to be up-scaled from 12 km, with the possibility of losing precise spatial information. The advantage of presenting 850 mb air temperature on its native grids allows the RCM to preserve high spatial details. Comparing modelled and reanalysis outputs on native grids were similarly employed by Lucas-Picher et al. (2016).

Figure 6 compares the averaged 1995 to 2014 mean December 850 mb air temperature from CRCM5 and reanalysis NARR outputs (Fig. 6a, b), respectively. The model output for December (Fig. 6a) seems to be slightly warmer along the southwestern tip of Lake Superior and northern Lake Huron, where the 265 K isotherm extends slightly farther north than the reanalysis output (Fig. 6b). In Fig. 6c, d, the same averaged 20-year duration is shown, but for January. Based on visual comparison, the CRCM5 captures well the 850-mb air temperature field over the GLB. The zonal isotherms are spatially aligned similarly between the CRCM5 and NARR.

The model also captures the colder southward air mass towards Lake Superior in January (Fig. 6c). Overall, there

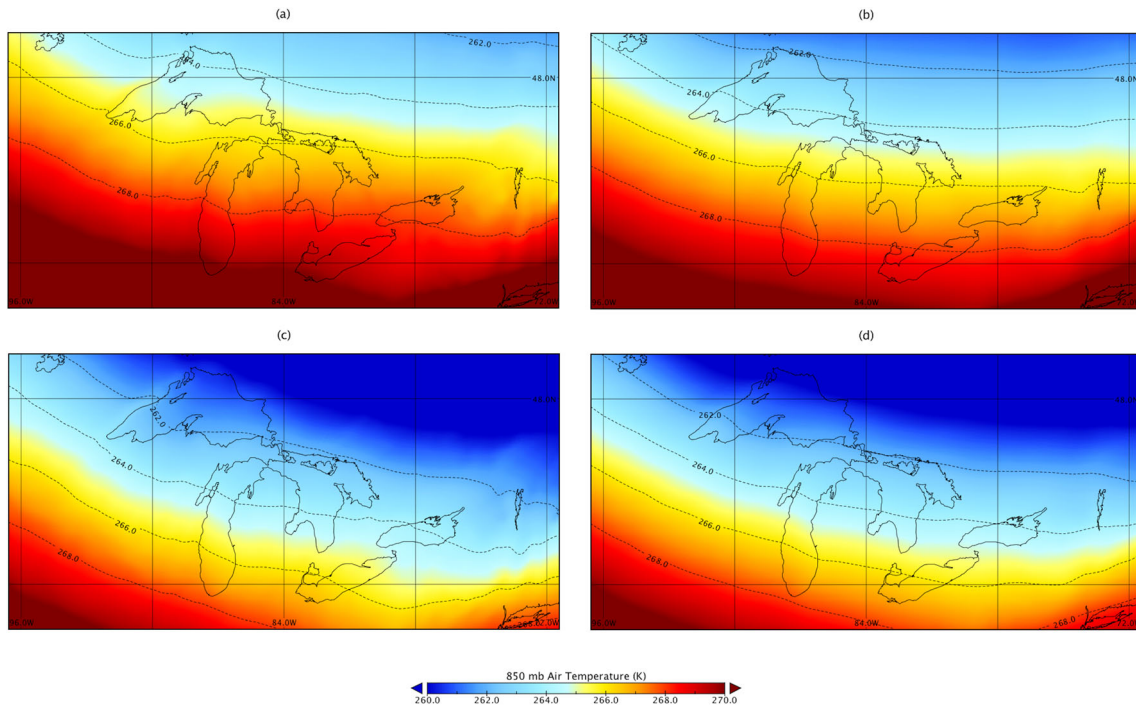


Fig. 6 Monthly mean 850 mb air temperature averaged over 1995–2014: **a** CRCM5 December mean, **b** NARR December mean, **c** CRCM5 January mean and **d** NARR January mean

are no strong biases in the 850-mb air temperature between the CRCM5 and reanalysis for the months of December and January. This is, perhaps, expected as both CRCM5 and NARR are driven by observed atmospheric reanalysis data forced at the lateral boundaries by ERA Interim and NCEP, respectively. These results are in agreement with Martynov et al. (2013) who analysed averaged 1989 to 2008 predicted 2-m air temperature from CRCM5 coupled with the FLake model and found that the air temperature is generally reproduced over the whole annual cycle for the Great Lakes region. Evident from the current research, the 850-mb air temperature over the Great Lakes has minimal discrepancies and, as a result, is not a factor that highly influences the modelled lake-induced snowfall biases. Other surface–atmosphere LES variables are explored to help determine the reasons for the aforementioned biases.

3.4 Surface predictor variables

Twenty-year time series are plotted for monthly mean of lake-wide averaged LST and ice cover concentration for both observations and simulation. Figure 7 presents the time series for Lake Superior for the month of December. Figure 7a shows the averaged lake-wide LST. Results indicate that the CRCM5 captures a similar pattern of the observed inter-annual variability, with a peak LST in 1998 and a local minimum in 2008. Although the simulated LST follows that of the observed, the simulated LST is evidently warmer. Table 3 shows that the RMSD of LST for Lake Superior, in December, is 2.13 and the MBD is 2.02, indicating that the RCM overestimates the LST.

In Fig. 7b, the lake-wide ice cover concentration is plotted. The simulated and observed inter-annual variability do not

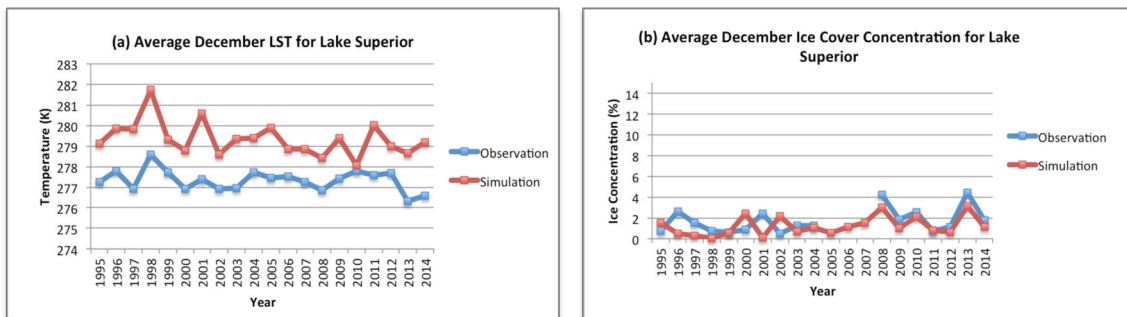


Fig. 7 1995 to 2014 time series of observed (blue) and simulated (red) December averaged **a** lake surface temperature and **b** ice cover concentration for Lake Superior

Table 3 Statistical comparison of observed versus simulated outputs of December's LST and ice cover concentration, for Lakes Superior and Huron

Variables	Root mean square difference (RMSD)		Mean bias difference (MBD)		
	December	Superior	Huron	Superior	Huron
LST		2.13	1.68	2.02	1.43
Ice cover		1.10	5.63	-0.36	-3.73

follow a similar pattern and show disagreements in peak ice cover years, from 1995 to 2004. For most years, the simulation shows lower ice cover concentrations than that of the observed, which could correspond to the warmer simulated LST temperatures. The RMSD is 1.10 with a negative MBD of 0.36, suggesting that the CRCM5 under-estimates ice cover (Table 3). The model's warmer LST and less ice cover over Lake Superior in December should, in theory, favour the production of LES along the leeward shores of Lake Superior. However, the 20-year averaged SWE and wintertime precipitation indicated a negative bias (recall Figs. 1 and 3).

Similarly, Fig. 8 plots the 20-year December time series of LST (Fig. 8a) and ice cover concentration (Fig. 8b), respectively, for Lake Huron. Table 3 shows that the RMSD and MBD are both larger for Lake Superior's LST than Lake Huron's. However, there is a greater disagreement between the simulation and observation for Lake Huron's ice cover compared to that of Lake's Superior, indicating that the simulation under-estimates ice cover for Lake Huron more than Lake Superior.

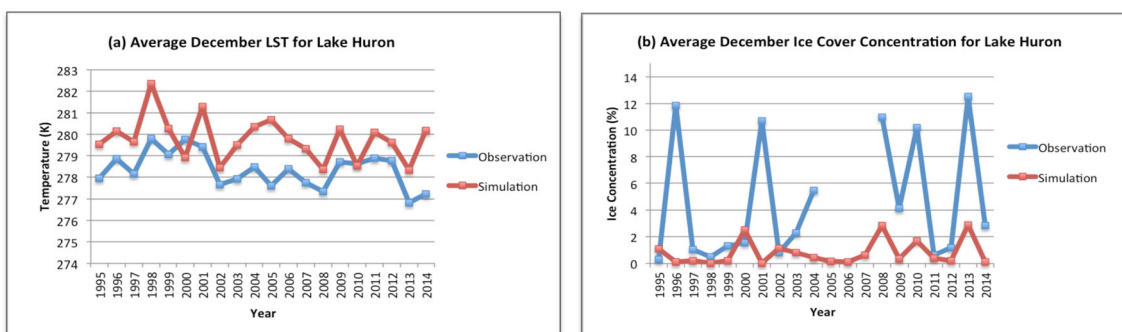
Figure 9 shows January's LST and ice cover for Lake Superior (Fig. 9a, b), respectively. Results show that the inter-annual variability for simulated Lake Superior's LST and ice cover are slightly over-estimated in January (Table 4). Figure 10a, b shows the inter-annual variability in lake-wide LST and ice cover for Lake Huron, respectively. There is a slight warmer bias in the model prediction for LST and an under-prediction in ice cover for Lake Huron. The biases in wintertime LST and ice cover are consistent with Martynov et al. (2012, 2013), who suggest that the FLake model over-estimates summertime temperatures for the Great Lakes, thereby leaving lakes free of ice for a longer

period, than that of observed, into the winter months and creating a warm wintertime bias. In the current study, for both lakes during both LES seasons, the model over-predicts the LST. Ice cover predictions correspond to the warmer bias in the model's LST, by under-estimating ice cover concentrations for both lakes, except for Lake Superior in January. Thus, the current results of the positive wintertime LST bias and negative ice cover bias, for the lakes, are in agreement with previous literature.

Validation studies by Martynov et al. (2013) also suggest that precipitation rates are well represented by the CRCM5 over the whole Great Lakes domain in the summertime but is over-estimated during the autumn and winter months for the 1989 to 2008 period. Furthermore, the over-estimation in precipitation can be attributed to enhanced evaporation from the overlying warm ice-free surface of the Great Lakes. While this may be the case for the overall GLB, the current study suggests that precipitation is under-estimated for the Canadian snowbelts of Lakes Superior and Huron between 1995 and 2014.

Wright et al. (2013) assessed the impacts of both LST and ice in the Weather Research and Forecasting Model (WRF) and found that the increased ice cover and thickness suppressed the formation of LES because increased ice cover is shown to decrease sensible and latent heat fluxes into the atmosphere (Gerbush et al. 2008; Zulauf and Krueger 2003). Warmer LST and lower ice cover should create high intensity and spatial cover of snowfall (Wright et al. 2013), relative to the observed results because lakes would be able to generate greater energy fluxes into the atmosphere.

It is suggested that sensible and latent heat fluxes' representation within the model could also affect the production of LES. Sensible and latent heat fluxes are of primary importance

**Fig. 8** 1995 to 2014 time series of observed (blue) and simulated (red) December averaged **a** lake surface temperature and **b** ice cover concentration for Lake Huron

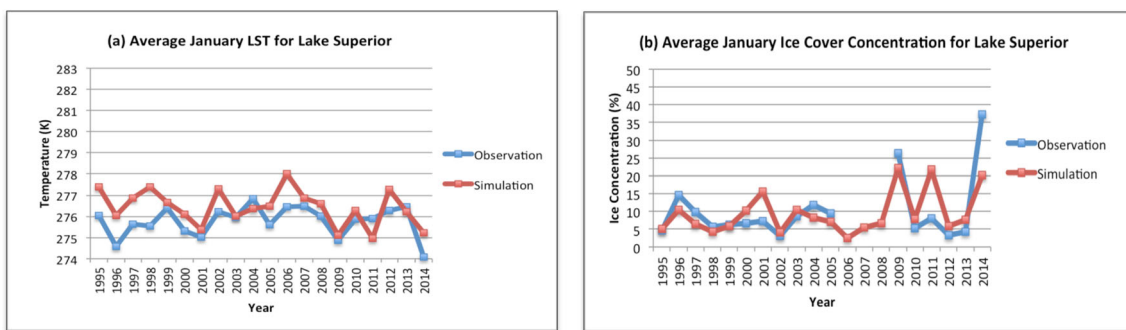


Fig. 9 1995 to 2014 time series of observed (blue) and simulated (red) January averaged **a** lake surface temperature and **b** ice cover concentration for Lake Superior

for the development of LES because a transfer of both heat and moisture from the lake into the lower PBL produces an unstable lapse rate at the lower levels and creates conditions favourable for convection. Lower PBL instability occurs because water vapour ($H_2O_{(g)}$) has a lower molecular weight than atmospheric oxygen ($O_{2(g)}$). Therefore, an increase in water vapour into the lower PBL decreases the density of the air mass and increases the instability of the air mass, inducing convection, development of cloud formation and lake effect precipitation. Furthermore, increased sensible and latent heat fluxes into the PBL increase both the air temperature and dew point temperature over the lake (Phillips 1972). As a result, convective available potential energy (CAPE) is increased within the above air parcel, inducing convection and cloud formation, which are favourable for the development of LES. Therefore, these fluxes are important key factors in influencing the production of LES.

Also, Lofgren and Zhu (2000) observed high outgoing sensible and latent heat fluxes over the late fall and early winter, which drive strong cooling of the lake surface and consequent convective mixing within the lake water column. However, while the epilimnion layer, in FLake, can account for convective and mechanical mixing, FLake does not represent these processes in the hypolimnion layer, which are present in large and deep lakes (Perroud et al. 2009; Balsamo et al. 2012; Mallard et al. 2014).

Thus, the large discrepancy in the predicted lake variables may be attributed to unrealistic parameterisation schemes within the FLake model. For example, sensible and latent heat fluxes are calculated in the CRCM5 lake interface module and are based on parameters supplied by the model, such as surface temperature and ice cover. Martynov et al. (2012)

explain that the influence of lakes on air temperature and humidity in lake-rich regions is weakly simulated in FLake. Kourzeneva (2010) suggests that a basic issue of lake parameterisation in numerical weather predictions and climate simulations is the need for external lake parameters and that the most important lake parameter is the minimum depth required for lake models. Thus, assigning a virtual depth of only 60 m for Lake Superior, which, in actuality, has a maximum lake depth of 406 m, could cause significant biases in lake thermal process simulations (Gu et al. 2015), because lake depth is a controlling factor influencing ice freeze-up and ice break-up dates (Duguay et al. 2003, 2006). Furthermore, FLake does not allow partial ice cover for each grid cell (Martynov et al. 2012); thus, local ice cover could be falsely represented, thereby influencing the production of localised lake-induced snowfall.

Although lake ice and temperature sensitivity analyses with FLake, conducted by Martynov et al. (2012), showed that FLake outperformed other one-dimensional lake prediction models over the Great Lakes, the one-dimensional models failed to capture patterns of springtime warming in the Great Lakes. This failure suggests the absence of three-dimensional processes, such as lake currents, ice drift and the formation of thermal bars (Wang et al. 2010; Bai et al. 2013), thereby negatively affecting the predictive capabilities of FLake (Mallard et al. 2014). The one-dimensional lake model, FLake, is interactively coupled to the CRCM5, and despite providing satisfactory predictions of temperature and ice cover, it is limited compared to three-dimensional dynamical lake models that could simulate both horizontal and vertical circulation (Lucas-Picher et al. 2016) and important deep convection that occurs twice a year (Bai et al. 2013). The quality of

Table 4 Statistical comparison of observed versus simulated outputs of January’s LST and ice cover concentration, for Lakes Superior and Huron

Variables	Root mean square difference (RMSD)		Mean bias difference (MBD)	
	Superior	Huron	Superior	Huron
LST	0.95	1.05	0.65	0.68
Ice cover	6.22	11.94	0.05	-9.79

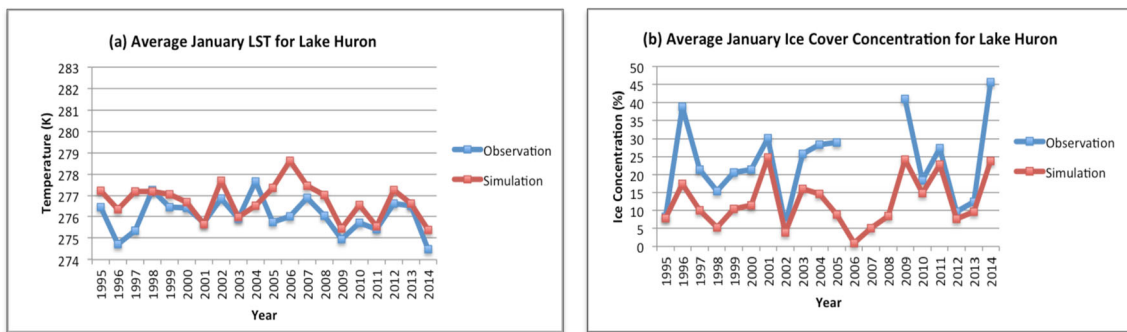


Fig. 10 1995 to 2014 time series of observed (blue) and simulated (red) January averaged **a** lake surface temperature and **b** ice cover concentration for Lake Huron

reproduced SWE, wintertime precipitation and lake-induced precipitation events along the Canadian leeward shores of Lake Superior and Lake Huron is, thus, highly dependent on the performance of FLake (Martynov et al. 2013).

4 Conclusions

The purpose of this study was to validate a regional climate model (CRCM5) in predicting snowfall along Canadian snowbelts of Lakes Superior and Huron within the Laurentian GLB. Gridded outputs of total December and January SWE and, separately, precipitation, were averaged over the 20-year period of 1995 to 2014. Gridded RMSD and MBD were computed between the model and interpolated gridded dataset (Daymet). Results showed that the CRCM5 under-estimates both SWE and precipitation along both snowbelts in December and January. The negative biases in SWE and precipitation along the shores of these Great Lakes suggest that the processes of lake-induced snowfall were not properly represented by the model.

In order to understand the sources of these biases, seven lake-induced events along Lake Superior or Lake Huron's snowbelt were selected for the months of December or January during a high and low ice season to validate the model's performance in capturing the timing, location and precipitation accumulation of each event. The results in this study showed that while the model generally predicted the onset of the squall bands and the general location of the trajected squall paths, it drastically under-estimated the daily total lake effect precipitation accumulation. The study further validated the model's capabilities in simulating LES predictor variables, which are key factors in the development of lake-induced precipitation.

The LES predictor variables included 850 mb air temperature, lake-wide LST, and lake-wide ice cover concentration (Xiao et al. 2017). Time series of the simulated outputs of LST and ice cover were plotted against the observed dataset for each variable. While the model accurately simulates 850 mb air temperature, it over-estimates LST for both lakes in December and

January, respectively. Ice cover is under-estimated in both lakes for December, but only for Lake Huron in January.

This study suggests limitations within the coupled simulation. The CRCM5 is interactively coupled to the one-dimensional FLake model, which is used to reproduce LST and ice cover concentration. The accuracy and precision of the simulated lake-induced events within the snowbelt regions of the Laurentian Great Lakes are highly dependent on the performance of the coupled lake model (Martynov et al. 2013). However, there are limitations within the one-dimensional FLake model, such as a virtual lake depth of only 60 m and the inability to simulate both horizontal and vertical circulation, deep convection processes that can be reproduced by three-dimensional dynamical lake models such as the Nucleus for European Modelling of the Ocean (NEMO) (Dupont et al. 2012; Durnford et al. 2018). In the future, as three-dimensional lake models become more available (Wang et al. 2010; Bai et al. 2013; Anderson et al. 2018), the interactive coupling of three-dimensional lake models to RCMs should be applied in order to assess the accuracy of LES forecasts.

Publisher's note Springer Nature remains neutral with regard to jurisdictional claims in published maps and institutional affiliations.

References

- Albritton DL, and et al. (2001) Summary for policy makers. Climate change 2001: the scientific basis, J. T. Houghton et al., Eds., Cambridge University Press. <http://www.ipcc.ch>
- Anderson E, Fujisaki-Manome A, Kessler J, Chu P, Kelley J, Lang G, Chen Y, Wang J (2018) Ice forecasting in the next-generation Great Lakes Operational Forecast System (GLOFS). *J Mar Sci Eng* 6:123. <https://doi.org/10.3390/jmse6040123>
- Anyah RO, Semazzi FHM (2004) Simulation of the sensitivity of Lake Victoria basin climate to lake surface temperature. *Theor Appl Climatol* 79:55–69
- Bai X, Wang J, Schwab DJ, Yang Y, Luo L, Leshkevich GA, Liu S (2013) Modeling 1993–2008 climatology of seasonal general circulation and thermal structure in the Great Lakes using FVCOM. *Ocean Model* 65:40–63. <https://doi.org/10.1016/j.ocemod.2013.02.003>

- Bajinath-Rodino JA, Duguay CR (2018) Historical spatiotemporal trends in snowfall extremes over the Canadian domain of the Great Lakes Basin. *Adv Meteorol*
- Bajinath-Rodino JA, Duguay CR, LeDrew E (2018) Climatological trends of snowfall over the Laurentian Great Lakes Basin. *Int J Climatol* 38:3942–3962. <https://doi.org/10.1002/joc.5546>
- Ballentine RJ, Stamm AJ, Chermack EF, Byrd GP, Schleede D (1998) Mesoscale model simulation of the 4–5 January 1995 lake-effect snowstorm. *Weather Forecast* 13:893–920
- Balsamo G, Salgado R, Dutra E, Boussetta S, Stockdale T, Potes M (2012) On the contribution of lakes in predicting near-surface temperature in a global weather forecasting model. *Tellus* 64:15829. <https://doi.org/10.3402/tellusa.v64i0.15829>
- Bates GT, Giorgi F, Hostetler SW (1993) Toward the simulation of the effects of the Great Lakes on regional climate. *Mon Weather Rev* 121:1373–1387
- Bates GT, Hostetler SW, Giorgi F (1995) Two-year simulation of the Great Lakes region with a coupled modeling system. *Mon Weather Rev* 123:1505–1522
- Baxter MA, Graves CE, Moore JT (2005) A climatology of snow-to-liquid ratio for the contiguous United States. *Weather Forecast* 20:729–744
- Burnett AW, Kirby ME, Mullins HT, Patterson WP (2003) Increasing Great Lake-effect snowfall during the twentieth century: a regional response to global warming? *J Clim* 16:3535–3542
- Cairns MM, Collins R, Cylke T, Deutschendorf M, Mercer D (2001) A lake effect snowfall in Western Nevada—part I: synoptic setting and observations. Paper presented at the 18th conference on weather analysis and forecasting/14th conference on numerical weather prediction, Fort Lauderdale
- Campbell LS, Steenburgh WJ, Veals PG, Letcher TW, Minder JR (2016) Lake effect mode and precipitation enhancement over the Tug Hill Plateau during OWELes IOP2b. *Mon Weather Rev* 144(5):1729–1748
- Carpenter DM (1993) The lake effect of the Great Salt Lake: overview and forecast problems. *Weather Forecast* 8(2):191–193
- Chow FK, Weigel AP, Street RL, Rotach MW, Xue M (2006) High resolution large eddy simulations of flow in a steep alpine valley. Part one: methodology, verification, and sensitivity experiments. *J Appl Meteorol Climatol* 45:63–86
- Cohen SJ, Allsopp TR (1988) The potential impacts of a scenario of CO₂-induced climatic change on Ontario, Canada. *J Clim* 1:669–681
- Cosgrove BA, Colucci RJ, Waldstreicher JS (1996) Lake effect snow in the Finger Lakes region. Preprints, 15th Conf. on weather analysis and forecasting, Norfolk, VA, American Meteorological Society: 573–576
- Dee DP, Uppala SM, Simmons AJ, Berrisford P, Poli P, Kobayashi S, Andrae U, Balmaseda MA, Balsamo G, Bauer P, Bechtold P, Beljaars ACM, van de Berg L, Bidlot J, Bormann N, Delsol C, Dragani R, Fuentes M, Geer AJ, Haimberger L, Healy SB, Hersbach H, Hólm EV, Isaksen I, Kållberg P, Köhler M, Matricardi M, McNally AP, Monge-Sanz BM, Morcrette JJ, Park BK, Peubey C, de Rosnay P, Tavolato C, Thépaut JN, Vitart F (2011) The ERA-Interim reanalysis: configuration and performance of the data assimilation system. *Q J R Meteorol Soc* 137(656):553–597. <https://doi.org/10.1002/qj.828>
- Duguay CR, Flato GM, Jeffries MO, Ménard P, Morris K, Rouse WR (2003) Ice covers variability on shallow lakes at high latitudes: model simulation and observations. *Hydrol Process* 17(17):3465–3483
- Duguay CR, Prose TD, Bonsal BR, Brown RD, Lacroix MP, Ménard P (2006) Recent trends in Canadian lake ice cover. *Hydrol Process* 20(4):781–801
- Dupont F, Chittibabu P, Fortin V, Rao YR, Lu Y (2012) Assessment of a NEMO-based hydrodynamic modelling system for the Great Lakes. *Water Qual Res J Can* 47(3–4):198. <https://doi.org/10.2166/wqrjc.2012.014>
- Durnford D, Fortin V, Smith GC, Archambault B, Deacu D, Dupont F, Dyck S, Martinez Y, Klyszejko E, MacKay M, Liu L, Pellerin P, Pietroniro A, Roy F, Vu V, Winter B, Yu W, Spence C, Bruxer J, Dickhout J (2018) Toward an operational water cycle prediction system for the Great Lakes and St. Lawrence River. *BAMS* 99:521–546. <https://doi.org/10.1175/BAMS-D-16-0155.1>
- ECCC (2017) Environment and Climate Change Canada, lake ice climatic atlas for the Great Lakes 1981–2010. Available online at <http://www.ec.gc.ca/glaces-ice/default.asp?lang=En&n=F1596609-1&offset=1&toc=show>. Accessed 9 Feb 2017.
- ECCC (2018) Environment and Climate Change Canada, glossary. Available online at http://climate.weather.gc.ca/glossary_e.html#t. Accessed 2018.
- Eichenlaub VL (1970) Lake effect snowfall to the lee of the Great Lakes: its role in Michigan. *BAMS* 51:403–412
- Eichenlaub, VL (1979) *Weather and climate of the Great Lakes region*. Notre Dame, Indiana: The University of Notre Dame Press
- Gerbush MR, Kristovich DAR, Laird NF (2008) Mesoscale boundary layer and heat flux variations over pack ice-covered Lake Erie. *J Appl Meteorol Climatol* 47:668–683
- Gu H, Jin J, Wu Y, Ek MB, Subin ZM (2015) Calibration and validation of lake surface temperature simulations with the coupled WRF-lake model. *Clim Chang* 129(3–4):471–483. <https://doi.org/10.1007/s110584-013-0978-y>
- Gula J, Peltier R (2012) Dynamical downscaling over the Great Lakes Basin of North America using the WRF regional climate model: the impact of the Great Lakes system on regional greenhouse warming. *J Clim* 25:7723–2242. <https://doi.org/10.1175/JCLI-D-11-00388.1>
- Hamilton RS, Saff D, Nizol T (2006) A catastrophic lake effect snow storm over Buffalo, NY October 12–14, 2006 case study. NOAA National Weather Service, Buffalo, NY. 22nd Conf. On Weather Analysis and Forecasting/18th Conf. on numerical weather prediction. [Available online at https://ams.confex.com/ams/22WAF18NWP/techprogram/paper_124750.htm]
- Hartmann H, Livingstone J, Stapleton MG (2013) Seasonal forecast of local lake-effect snowfall: the case of Buffalo, USA. *Int J Environ Res* 7(4):859–867
- Holroyd EW III (1971) Lake effect cloud bands as seen from weather satellites. *J Atmos Sci* 28(7):1165–1170
- Hostetler SW (1991) Simulation of lake ice and its effect on the late-Pleistocene evaporation rate of Lake Lahontan. *Clim Dyn* 6:43–48
- Hostetler SW (1995) Hydrological and thermal response of lakes to climate: description and modeling. In: Lerman A, Imboden D, Gat J (eds) *Physics and chemistry of lakes* (pp. 63–82). Springer, Berlin
- Hostetler SW, Bartlein PJ (1990) Modeling climatically determined lake evaporation with application to simulating lake-level variations of Harney-Malheur Lake, Oregon. *Water Resour Res* 26:2603–2612
- Hostetler SW, Bates GT, Giorgi F (1993) Interactive coupling of a lake thermal model with a regional climate model. *J Geophys Res* 98:5045–5057
- Hozumi K, Magono C (1984) The cloud structure of convergent cloud bands over the Japan Sea in winter monsoon period. *J Meteorol Soc Jpn* 62(3):522–533
- Kalnay E et al (1996) The NCEP/NCAR 40-year reanalysis project. *BAMS* 77:437–471
- Kheyrollah Pour, H, Duguay CR, Martynov A, Brown LC (2012) Simulation of surface temperature and ice cover of large northern lakes with 1-D models: a comparison with MODIS satellite data and in situ measurements. *Tellus A* 64, doi: <https://doi.org/10.3402/tellusa.v64i0.17614>
- Kourzeneva EP (2010) External data for lake parameterization in numerical weather prediction and climate modeling. *Boreal Environ Res* 15:165–177

- Kourzeneva EP, Samuelsson P, Ganbat G, Mironov D (2008) Implementation of lake model Flake into HIRLAM. HIRLAM Newsletter, 54: 54–64. [Available http://hirlam.org/index.php/component/docman/doc_view/195-hirlam-newsletter-no-54-paper-07-kourzeneva]
- Kristovich DAR, Laird NF (1998) Observations of widespread lake effect cloudiness: influence of lake temperature and upwind conditions. *Weather Forecast* 13:811–821
- Kristovich DAR, Spinar ML (2005) Diurnal variations in lake-effect precipitation near western Great Lakes. *J Hydrometeorol* 6(2):210–218
- Kunkel KE, Wescott NE, Kristovich DAR (2000) Climate change and lake effect snow. Preparing for a changing climate: the potential consequences of climate variability and change. *J Great Lakes Res* 28:521–536
- Kunkel KE, Wescott NE, Kristovich DAR (2002) Assessment of potential effects of climate change on heavy lake-effect snowstorms near Lake Erie. *J Great Lakes Res* 28(4):521–536
- Laird NF, Desrochers J, Payer M (2009) Climatology of lake-effect precipitation events over Lake Champlain. *J Appl Meteorol Climatol* 48(2):232–250
- Laird NF, Sobash R, Hodas N (2010) Climatological conditions of lake-effect precipitation events associated with the New York State Finger Lakes. *J Appl Meteorol Climatol* 49:1052–1062. <https://doi.org/10.1175/2010JAMC2312>
- Laprise R (1992) The Euler equation of motion with hydrostatic pressure as independent coordinate. *Mon Weather Rev* 120:197–207
- Leathers DJ, Ellis AW (1993) Relationships between synoptic weather type frequencies and snowfall trends in the lee of Lakes Erie and Ontario. Proceedings, 61st annual western snow conference, Quebec City, Canada, CRREL, 325–330
- Leathers DJ, Ellis AW (1996) Synoptic mechanisms associated with snowfall increases to the lee of Lakes Erie and Ontario. *Int J Climatol* 16:1117–1135
- Lo JF, Yang ZL, Pielke RA Sr (2008) Assessment of three dynamical climate downscaling methods using the weather research and forecasting (WRF) model. *J Geophys Res* 113. <https://doi.org/10.1029/2007JD009216>
- Lofgren BM, Zhu Y (2000) Surface energy fluxes on the Great Lakes based on satellite-observed surface temperatures 1992 to 1995. *J Great Lakes Res* 26(4):305–314
- Lucas-Picher P, Laprise R, Winger K (2016) Evidence of added value in North American regional climate model hindcast simulations using ever-increasing horizontal resolutions. *Clim Dyn* 48:2611–2633. <https://doi.org/10.1007/s00382-016-3227-z>
- Mallard MS, Nolte CG, Bullock OR, Spero TL, Gula J (2014) Using a coupled lake model with WRF for dynamical downscaling. *J Geophys Res-Atmos* 119:7193–7208. <https://doi.org/10.1002/2014JD021785>
- Martynov A, Laprise R, Sushama L (2008) Off-line lake water and ice simulations: A step towards the interactive lake coupling with the Canadian Regional Climate Model. Geophysical Research Abstract, 10, EGU2008-A-02898, EGU General Assembly, Vienna, Austria
- Martynov A, Sushama L, Laprise R (2010) Simulation of temperate freezing lakes by one-dimensional lake models: performance assessment for interactive coupling with regional climate models. *Boreal Environ Res* 15:143–164
- Martynov A, Sushama L, Laprise R, Winger K, Dugas B (2012) Interactive lakes in the Canadian Regional Climate Model, version 5: the role of lakes in the regional climate of North America. *Tellus* 64:16226. <https://doi.org/10.3402/tellusa.v64i0.16226>
- Martynov A, Laprise R, Sushama L, Winger K, Separovic L, Dugas B (2013) Reanalysis-driven climate simulation over CORDEX North America domain using the Canadian Regional Climate Model, version 5: model performance evaluation. *Clim Dyn* 41:2973–3005
- Menne MJ, Durre I, Vose RS, Gleason BE, Houston TG (2012) An overview of the global historical climatology network-daily database. *J Atmos Ocean Technol* 29(7):897–910
- Mesinger F (2006) North American regional reanalysis. *BAMS* 87:343–360
- Mironov DV (2008) Parameterization of lakes in numerical weather prediction, description of a lake model, COSMO. Technical Report No. 11. (pp. 41). Deutscher Wetterdienst, Offenbach am Main, Germany
- Mironov D, Heise E, Kourzeneva E, Ritter B, Schneider N, Terzhevik A (2010) Implementation of the lake parameterisation scheme FLake into the numerical weather prediction model COSMO. *Boreal Environ Res* 15:218–230
- Niziol TA (1987) Operational forecasting of lake effect snow in western and central New York. *Weather Forecast* 2(4):310–321
- Niziol TA, Snyder WR, Waldstreicher JS (1995) Winter weather forecasting throughout the Eastern United States, part 4: lake effect snow. *Weather Forecast* 10:61–77
- NOAA GLERL, National Oceanic and Atmospheric Administration, Great Lakes Environmental Research Laboratory, 2017: About our lakes. Accessed 15 January 2017. [Available online at <https://www.glerl.noaa.gov/education/ourlakes/intro.html>]
- Norton D, Bolsenga S (1993) Spatiotemporal trends in lake effect and continental snowfall in the Laurentian Great Lakes, 1951–1980. *J Clim* 6:1943–1956. [https://doi.org/10.1175/1520-0442\(1993\)006<1943:STILEA>2.0.CO;2](https://doi.org/10.1175/1520-0442(1993)006<1943:STILEA>2.0.CO;2)
- Notaro M, Zarrin A, Fluck E, Vavrus S, Bennington V (2013a) Influence of the Laurentian Great Lakes on regional climate. *J Clim* 26:789–804. <https://doi.org/10.1175/JCLI-D-12-00140.1>
- Notaro M, Zarrin A, Vavrus S, Bennington V (2013b) Simulation of heavy lake-effect snowstorms across the Great Lakes Basin by RegCM4: synoptic climatology and variability. *Mon Weather Rev* 141:1990–2014
- Obolkin VA, Potemkin VL (2006) The impact of large lakes on climate in the past: a possible scenario for Lake Baikal. *Hydrobiologia* 568: 249–252
- Payer M, Desrochers J, Laird NF (2007) A lake-effect snowband over Lake Champlain. *Mon Weather Rev* 135(11):3895–3900
- Pease SR, Lyons WA, Keen CS, Hjelmfelt MR (1988) Mesoscale spiral vortex embedded within a Lake Michigan snow squall band: high resolution satellite observations and numerical model simulations. *Mon Weather Rev* 116:1374–1380
- Perroud MS, Goyette S, Martynov A, Beniston M, Anneville O (2009) Simulation of multiannual thermal profiles in deep Lake Geneva: a comparison of one-dimensional lake models. *Limnol Oceanogr* 54: 1574–1594
- Phillips DW (1972) Modification of surface air over Lake Ontario in winter. *Mon Weather Rev* 100(9):662–670
- Samuelsson P, Kourzeneva E, Mironov D (2010) The impact of lakes on the European climate as simulated by a regional climate model. *Boreal Environ Res* 15:113–129
- Scott AK, Buehner M, Caya A (2012) Assimilation of AMSR-E brightness temperatures for estimating sea ice concentration. *Mon Weather Rev* 140:997–1013. <https://doi.org/10.1175/MWR-D-11-00014.1>
- Semmler T, Cheng B, Yang Y, Rontu L (2012) Snow and ice on Bear Lake (Alaska)—sensitivity experiments with two lake ice models. *Tellus A* 64:17339. <https://doi.org/10.3402/tellusa.v64i0.17339>
- Theeuwes NE, Steeneveld GJ, Krieken F, Holtslag AM (2010) Mesoscale modeling of lake effect snow over Lake Erie—sensitivity to convection, microphysics and the water temperature. *Adv Sci Res* 4:15–22
- Thornton PE, Running SW, White MA (1997) Generating surfaces of daily meteorological variables over large regions of complex terrain. *J Hydrol* 190:214–251
- Thornton PE, Hasenaur H, White MA (2000) Simultaneous estimation of daily solar radiation and humidity from observed temperature and

- precipitation: an application over complex terrain in Austria. *Agric For Meteorol* 14:255–271
- Thomton PE, Thornton MM, Mayer BW, Wei Y, Devarakonda R, Vose RS, Cook RB (2016) Daymet: daily surface weather data on a 1-km grid for North America, Version 3. ORNL DAAC, Oak Ridge Tennessee, USA. Accessed January, 2018. [Available online <https://doi.org/10.3334/ORNLDAAAC/1328>]
- Vavrus S, Notaro M, Zarrin A (2013) The role of ice cover in heavy lake-effect snowstorms over the Great Lakes Basin as simulated by RegCM4. *Mon Weather Rev* 141:148–165
- Verseghy DL (2009) CLASS—the Canadian land surface scheme (version 3.4)—technical documentation (version 1.1). (pp.183). Internal report. Climate Research Division, Science and Technology Branch, Environment Canada
- Wang J, Hu H, Schwab D, Leshkevich G, Beletsky D, Hawley N, Clites A (2010) Development of the Great Lakes ice-circulation model (GLIM): application to Lake Erie in 2003–2004. *J Great Lakes Res* 36:425–436. <https://doi.org/10.1016/j.jglr.2010.04.002>
- Wang J, Assel RA, Walterscheid S, Clites A, Bai X (2012) Great lakes ice climatology update: winter 2006 – 2011 description of the digital ice cover data set, NOAA Technical Memorandum GLERL-155, 37 pp. 2012
- Wang J, Kessler J, Hang F, Hu H, Clites AH, Chu P (2017) Analysis of Great Lakes ice cover climatology: winters 2012–2017, NOAA Technical Memorandum GLERL-171, 15 pp. 2017
- Wang J, Kessler J, Bai X, Assuncao A, Clites A, Lofgren B, Bratton J, Chu P, Leshkevich G (2018) Decadal variability of Great Lakes ice cover in response to AMO and PDO, 1963–2017. *J Clim* 31:7249–7268. <https://doi.org/10.1175/JCLI-D-17-0283.1>
- Wiggin BL (1950) Great snows of the Great Lakes. *Weatherwise* 3:123–126
- Wright DM, Posselt DJ, Steiner AL (2013) Sensitivity of lake effect snowfall to lake ice cover and temperature in the Great Lakes region. *Mon Weather Rev* 141:670–689. <https://doi.org/10.1175/MWR-D-12-00038.1>
- Xiao C, Lofgren BM, Wang J, Chu PY (2017) Improving the lake scheme within a coupled WRF-lake model in the Laurentian Great Lakes. *JAMES* 8:1969–1985. <https://doi.org/10.1002/2016MS000717>
- Zadra A, Caya D, Ducas B, Jones C, Laprise R, Winger K, Caron L-P (2008) The next Canadian regional climate model. *Can J Phys* 64(2): 74–83
- Zulauf MA, Krueger SK (2003) Two-dimensional cloud-resolving modeling of the atmospheric effects of Arctic leads based upon midwinter conditions at the surface heat budget of the Arctic Ocean ice camp. *J Geophys Res* 108:4312. <https://doi.org/10.1029/2002JD002643>